JOURNAL OF CATALYSIS **179,** 1–17 (1998)
ARTICLE NO. CA982211

Synthesis, Characterization and Activity Studies of Carbon Supported Platinum Alloy Catalysts

S. T. Srinivas[1] and P. Kanta Rao

Indian Institute of Chemical Technology, Hyderabad 500 007, India

Received September 18, 1997; revised June 16, 1998; accepted June 16, 1998

A series of Pt-*M* (*M* = Cr, V, Zr) on carbon catalysts have been prepared using organometallic precursors. The catalysts were subjected to high temperature heat treatment to yield a supported alloy. The catalysts were characterized by XRD, ESR, chemisorption of CO, H_2, O_2, and NH_3 and BET surface area. The catalysts were evaluated for vapor phase hydrogenation of phenol and benzene. The thioresistance level of these alloy catalysts was studied for benzene hydrogenation reaction. Alloy formation was confirmed by X-ray diffraction analysis. The characterization shows that the catalysts used here were alloys, with some platinum exposed, covered by MO_x (M = Cr, V, Zr) species. The addition of the second metal suppresses chemisorption, but that oxygen and ammonia adsorption increased with the addition of the second metal. It was also observed that hydrogenation activity is increased when compared with Pt/C catalyst. The catalysts were highly selective either for cyclohexanone or cyclohexanol in phenol hydrogenation reaction. The alloy catalysts exhibited high thiotolerance level when compared to a Pt/C catalyst.

INTRODUCTION

Addition and alloying of platinum with a second metal has become a common practice in order to synthesize a catalyst with characteristics superior to those of the respective monometallic catalysts (1–7). Many state of the art industrial catalysts are a complicated mixture of at least two metals plus one or several dopants. Platinum alloy catalysts are not only commercially important but are also attractive objects for scientific studies. Recently studies have been performed on the preparation, characterization, and catalytic activity of supported alloy catalysts in which platinum is alloyed with d-block elements such as titanium, zirconium, etc. (8,9). These types of supported alloy catalysts have been investigated primarily in the form of electrocatalysts for phosphoric acid fuel cells (10,11).

The nature and composition of the supported alloy catalyst strongly depends on the way by which it is prepared. A general method of preparation employed is the coimpregnation or step impregnation of metallic salt precursors on the support (12,13). The catalyst can also be prepared by exchange of carrier surface with solutions of metallic salts. Recently a new route is receiving attention that involves the addition of the second metal as an organometallic compound to a prereduced monometallic catalyst (14,15). This can proceed via gas phase or liquid phase, depending on the nature of constituent elements. A unique feature of this method is the very selective metal organometallic interaction. This can be achieved because of controlled surface reaction (CSR) taking place between the carrier surface (i.e., monometallic catalyst) and the organometallic precursor.

Selective chemisorption of gases on a supported bimetallic system, where one bimetallic component strongly adsorbs the gas while the other adsorbs either weakly or not at all, is a good way to either obtain individual metal dispersions or assess the effect of one metal on the strength of adsorption of a gas on the other metal. The advantages of using multiple adsorbates to probe the catalytic surface has been reported (16). In bimetallic platinum catalysts one can determine platinum dispersion by selective chemisorption of gases. This is facilitated because platinum selectively adsorbs significant amounts of H_2, CO, or O_2 at room temperature with well-known chemisorption stochiometries, whereas that is not the case with most of the addition metals. From these considerations it appeared of great interest to extend the relevance of these concepts to our work.

The catalytic hydrogenation of aromatic hydrocarbons is a subject of continuous interest from both industrial and academic standpoints (17). The selective hydrogenation of substituted benzenes is a key step in the preparation of various industrially important intermediates (17). Addition of metallic salts to the reaction medium has been known for a long time to increase the selectivity of platinum catalysts. Alternatively, platinum catalysts must be promoted by the addition of metallic salts or by alloying (18,19). Bimetallic

[1] To whom correspondence should be addressed. Present address: Fuel Science Program and Laboratory for Hydrocarbon Process Chemistry, The Energy Institute, Pennsylvania State University, 209 Academic Projects Building, University Park, PA 16802, USA.

0021-9517/98 $25.00

or alloy catalysts possesses much longer lifetimes and a higher activity than platinum-only catalysts; however, the mode of action of these additives remains obscure. It is still not established whether they are fixed on the base metal or act as ensemble sites (20). The nature and texture of the support and the morphology of the metal particles also influence the selectivity of the catalyst. Phenol hydrogenation is an important reaction. Cyclohexanone, one of the products in this reaction is an important intermediate in the production of caprolactam for nylon-6 and adipic acid for nylon-66 (21). Cyclohexanone is manufactured by dehydrogenation of cyclohexanol using Cu-based catalysts or air oxidation of cyclohexane or by phenol hydrogenation (22). Usually phenol hydrogenation is carried out in liquid phase and is a two-step reaction. Hydrogenation of phenol over a Ni catalyst gives cyclohexanol selectively which on dehydrogenation over a Cu or Zn catalyst yields cyclohexanone. Recently Montedipe and Johnson-Matthey (23) developed a process based on promoted Pd/Al_2O_3 catalyst for single step vapor phase hydrogenation of phenol to give cyclohexanone, which is advantageous, where endothermic step of cyclohexanol dehydrogenation can be avoided.

In this paper the effect of alloying of Pt to Cr, V, or Zr on the adsorptive and activity behavior of carbon-supported platinum is explored for a series of platinum–alloy catalysts prepared by using organo metallic compounds. The catalysts were characterized by CO, H_2, O_2, and NH_3 chemisorption, X-ray diffraction, and electron spin resonance spectroscopy. The platinum alloy catalysts were evaluated for their activity in vapor phase hydrogenation of phenol. A complementary study of their reaction behavior in benzene hydrogenation was also made. Correlations between the physicochemical characteristics of platinum–alloy catalysts and activity data were made wherever possible.

EXPERIMENTAL

Catalyst Preparation

The base catalyst, 5 wt% Pt/carbon was prepared by incipient wetting of VULCAN XC-72 carbon (sulfur and iron free) with aqueous solution of hexachloro platinic acid, $H_2PtCl_6 \cdot 6H_2O$ (Fluka). The detailed preparation procedure is given elsewhere (24). The alloy catalysts (PtCr, PtV, and PtZr) were prepared by using the organometallic precursors namely chromium acetyl acetonate, vanadium acetyl acetonate, and zirconium isopropoxide (all Fluka) to deposit Cr, V, and Zr respectively on 5 wt% Pt/carbon. The base catalyst (5 wt% Pt/C) was prereduced at 400°C, cooled in flowing H_2 to room temperature and then purged with N_2. It was then maintained in contact for 24 h at 25°C with calculated amounts of Cr $(C_5H_7O_2)_3$, or V $(C_5H_7O_2)_3$, or $(C_{12}H_{28}O_{24})$ Zr in methanol to yield 0.5–4 wt% Cr, V, and Zr, as the case may be. The samples were then dried at 120°C for 6 h and were annealed at different temperatures (for PtCr, 760°C; Pt-V, 960°C; and PtZr, 1200°C) in flowing $H_2 : N_2$ (1 : 1) gas mixture (rate = 40 ml $\cdot$ min^{-1}) for 6 h. The annealing temperature for Pt-Cr/C (760°C), Pt-V/C (960°C), and Pt-Zr/C (1200°C) were selected on the basis of the phase diagrams showing the solubility of individual metal constituents, i.e., Pt-Cr, Pt-V, and Pt-Zr, to obtain ordered alloy phases in the prepared catalysts. After completion of heat treatment $H_2 : N_2$ mixture was replaced by N_2 and the sample was left to cool to room temperature. The base catalyst, Pt/C was also reduced at 760, 960, and 1200°C in flowing $H_2 : N_2$ (1 : 1) gas mixture (rate = 40 ml $\cdot$ min^{-1}) for 6 h for comparison with Pt-alloy catalysts. All the catalyst samples after heat treatment were collected in sample bottles and kept in a desiccator until used.

Chemical Analysis

The platinum content in the monometallic catalyst and Pt, Cr, V, and Zr contents in alloy catalysts were determined by inductively coupled plasma analysis (ICP) (Labtam Instruments, Australia). For ICP analysis about 0.5 g of catalyst sample was dissolved in a 3 : 1 mixture of concentrated HCl and HNO_3 (aquaregia) and digested for 1 h on a hot plate. The resulting slurry was filtered, washed with deionised water, and made up to a definite volume. From the ICP analysis the active components (Pt and Cr, V, and Zr, respectively) loading fell within the range of $=$0.005 wt% variation of the theoretical value.

X-Ray Diffraction (XRD)

X-ray diffraction was used to confirm alloying between constituent elements in the catalysts. XRD patterns of Pt/C catalyst reduced at different temperatures were also obtained. A Phillips X-ray diffractometer (PW-1051) with nickel filtered CuKα radiation was used for X-ray diffraction studies of the samples. The tube voltage was 40 KV, current was 45 mA, and the scanning rate was 20°/min. Every sample was carefully ground and fully packed into the XRD cell. The crystallite sizes of various samples were calculated from maximum intensity peak by using the scherrer relationship:

$$D_{hkl} = \frac{K - \lambda}{B_{hkl} \cos\theta}.$$

B_{hkl} is the width of the peak at half the peak maximum corrected for both the effect of K_1-K_2 separation and instrumental broadening (K_1 an K_2 are constants) was obtained directly from the pattern-fitting procedure applied; as a consequence the instrumental broadening accounted for assuming a Cauchy relationship (25).

Electron Spin Resonance (ESR)

ESR spectra of these samples were recorded on a Bruker ER 200 D-SRC X-band spectrometer with 100 KHz

modulation at room temperature. The catalyst sample to be studied was placed in a U tube attached with a graded seal which was then connected to a high vacuum system and was degassed to 10^{-6} torr pressure at 200°C for 6 h. The sample was cooled to room temperature under vacuum and then detached from the high vacuum apparatus. Only the Pt-V/C catalysts had an ESR signal.

Chemisorption Studies

A conventional Pyrex glass high vacuum system having a stationary background vacuum of 10^{-6} torr (1 torr = 133.3 Pa), with a facility to reduce the sample *in situ* by flowing hydrogen, was used in all chemisorption experiments. In a typical experiment the catalyst sample (ca 0.5 g) was placed in a U-shaped glass adsorption cell and was reduced by flowing hydrogen (40 ml/min) at 500°C for 4 h for platinum–alloy catalysts and 250°C for 6 h for a monometallic catalyst. The Pt/C catalyst reduced at 760, 960, and 1200°C was also pretreated at 250°C before carrying out chemisorption experiments. Reduction at 250°C in the case of platinum–alloy catalysts was found to be insufficient in our preliminary investigations. After evacuating the sample at the pretreatment temperature the sample was cooled under dynamic vacuum to room temperature (25°C), where the chemisorption measurements were made. The chemisorption isotherms were generated by using the following gases: H_2, O_2, CO, and NH_3 (Matheson, USA). The amount of chemisorbed gas on the catalyst sample was determined after discounting the physisorption. The experimental details of these adsorption methods are well established and reported and the same were adopted in this study (26). The BET surface areas of the samples before and after alloying, i.e., for impregnated samples and heat treated ones, were measured by adsorption of N_2 at −196°C, assuming 0.162 nm^2 as the area of cross section of the N_2 molecule. In case of BET surface areas measured after alloying the sample was saved after chemisorption experiments and was evacuated for several hours before the N_2 adsorption.

Activity Studies

A fixed-bed microcatalytic reactor was employed to carry out the phenol hydrogenation reaction. About 0.3 g of the catalyst sample was taken in the reactor (length = 20 cm, diameter = 12 mm) and kept between two quartz wool plugs. The sample was pretreated at 500°C for 2 h in hydrogen (40 ml/min) and then cooled to reaction temperature (200°C). In case of Pt/C catalyst reduced at different temperatures, the samples were pretreated at 250°C for 2 h in hydrogen (40 ml/min) and then cooled to 200°C. The reactant feed consisting of phenol dissolved in cyclohexane (1 : 4 wt/wt) with a hydrogen to phenol mole ratio of 4.7, was fed into the reactor using a microprocessor controlled Secura (B. Braun, Germany) syringe pump. The reaction products were condensed in cold traps after steady state conditions were attained (2 h) and were analyzed by GLC using 30% SE-30 on chromosorb W column and flame ionization detecter.

A vertical flow microreactor (length = 20 cm, diameter = 8 mm) operating under normal atmospheric pressure and interfaced with GC by a six-way gas sampling valve was used to study the catalytic properties of the catalysts in benzene hydrogenation. For each run about 0.2 g of the catalyst was prereduced in H_2 (40 ml/min) at 500°C for 2 h and then benzene + hydrogen feed was introduced to the reactor by means of bubblers kept at 30°C. In case of Pt/C catalyst reduced at different temperatures, the samples were pretreated at 250°C in H_2 (40 ml/min) for 2 h. The reaction product obtained was only cyclohexane and was analyzed by GC using a 10% carbowax 20 *M* on a chromosorb W column and flame ionization detector. Sulfur resistance behaviour of platinum alloy catalysts was also carried out in benzene hydrogenation. For the sulfur resistance study benzene was contaminated by carbon disulfide (14 ppm). Throughout this reaction benzene (Baker AR grade, thiophene free) with 99.9 purity was used.

RESULTS AND DISCUSSION

X-ray Diffraction (XRD)

In X-ray diffractograms of Pt/C catalyst reduced at different temperatures showed no characteristic peaks due to platinum at 250 and 400°C, indicating that at these reduction temperatures platinum is in an X-ray amorphous state. Peaks due to Pt (111) and Pt (200) (27) were observed at 760, 960, and 1200°C and peak intensities increased with the increase in reduction temperature. This observation showed that significant sintering of Pt/C catalyst has occurred, resulting in an increase in platinum crystallinity with the increasing temperature.

X-ray diffraction was used to detect alloying between platinum and the second metal in the catalysts. The X-ray patterns of Pt-Cr/C catalysts are presented in Fig. 1. It can be seen from the figure that peaks due to Pt(111) and Cr_3Pt ordered alloy phase are present in the X-ray patterns of Pt-Cr/C alloy catalysts (28). Sample PR-1 with a low Cr loading of 0.5 wt% is X-ray amorphous. Above 0.5 wt% Cr loading the peak intensity increases with the increase in Cr loading, although the peaks are broad in nature. A small but observable shift can be seen with respect to Pt(111) plane. This can perhaps be explained only as a consequence of a partial substitution of the platinum atoms by the chormium atoms, which are about 10% smaller, i.e. by the formation of a fcc Pt-Cr solid solution phase. In our opinion an essential reason for the possible reduction of $(CrO)_x$ species to metal in the presence of platinum which occurs at comparably low temperatures is that much more favorable thermodynamic conditions prevail at the heat treatment temperature. By mutual promotion and co-reduction

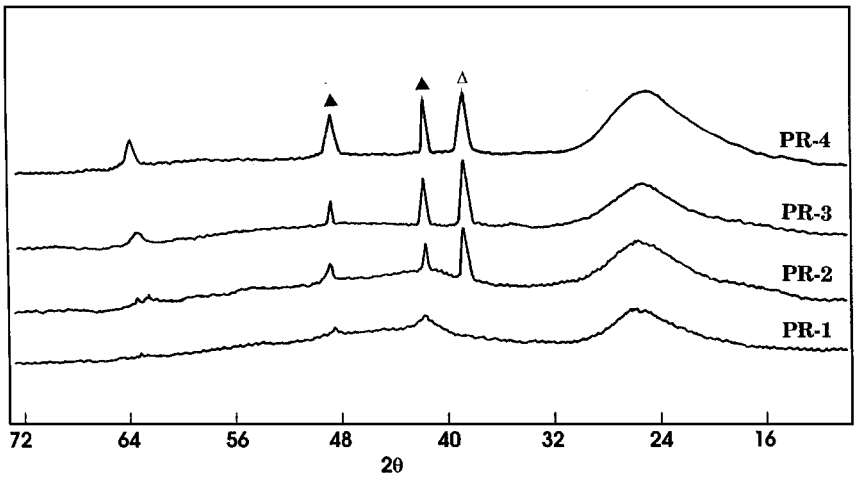

FIG. 1. X-ray diffraction patterns of Pt-Cr/C catalysts reduced at 760°C: Pt (▲), Cr_3Pt (△).

under the formation of a solid platinum–chromium solution no intermediate stabilization of low-grade oxidation states takes place. Engels and co-workers (29) from TPR experiments found evidence for such a co-reduction of Pt and chromium. They also found that the attainment of Cr° is linked to the stabilization of the Pt (FCC) metal phase achieved with the alloy formation and cannot be attributed to a H_2 spillover of the platinum during reduction step. Unlike in Pt-Cr/Al_2O_3 we did not observe any phases due to α -Cr_2O_3 in Pt-Cr/C catalysts. Joyner *et al*. (4,30) proposed a model for Pt-Cr metal alloy in zeolites in which the outer most monolayer consists entirely of platinum and the second shell, is enriched in the additive metal, chromium. Both XPS and XANES indicated a two-step reduction of Cr (VI) to Cr (111) and Cr (O) states, while analysis of EXAFS data demonstrates the formation of Pt-Cr alloy particles at a reduction temperature of 550°C.

X-ray patterns of Pt-V/C alloy catalysts are depicted in Fig. 2. In the pattern of PV-1 (wt%, V = 0.5) a broad band due to Pt_3V can be seen (31). In other samples strong reflections due to PtV_3 and PtV-ordered alloy phases could be seen (31). The reflection due to PtV_3 and PtV increased with the increase in vanadium loading. The formation of superstructures can be seen in PV-2 (wt%, V = 1.0) and PV-3 (wt%, V = 2.0) patterns. The existence of ordered intermetallic compound demonstrate that Pt-V bonding is stronger than V-V bonding so vanadium aggregation will not be favored at equilibrium. This is possible because of the relatively high temperatures used for reduction, which should allow efficient mixing of Pt and V in the catalyst. XRD patterns of Pt-V catalysts show that Pt(111) planes exhibited a shift with respect to a 5% Pt/C catalysts reduced at 800°C. From Fig. 2 it can be seen that the shift is in the increasing diffraction angle, that is smaller lattice spacings. A contraction in the lattice spacing indicates that vanadium is dissolving in platinum. It appears that the lattice spacing decreases with increasing vanadium content in the catalysts. The lattice spacings are consistent with a solid

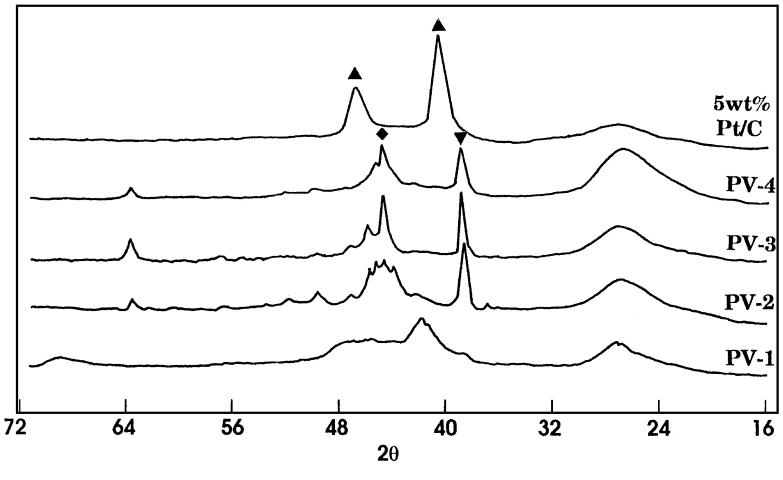

FIG. 2. X-ray diffraction patterns of 5 wt% Pt/C and Pt-V/C catalysts reduced at 960°C: PtV (▼), PtV_3 (◆).

solution Pt-V alloy with an indication that the vanadium concentration in the alloy may be less than that expected from the vanadium content of the catalysts. It is possible that even if intermetallic phase Pt_3V is formed it may be X-ray amorphous in nature. However, the intensity ratio of the strongest reflections from the catalysts is in good agreement with that for PtV_3 and PtV, rather than Pt_3V. Small peaks due to carbon vanadium oxides were also observed, indicating that some of the VO_x species in the sample are partially reduced, despite the promotion of reduction by platinum. Cambins and Chadwick (32) found from XPS analysis of Pt-V/C alloy catalysts that substantial quantities of vanadium oxide exist in the catalysts. It was suggested that the promotion of vanadium is associated with alloying while the formation of excessive surface vanadium oxide is tentatively seen as responsible for the fall in activity at high vanadium loadings.

In the case of Pt-Zr alloying the driving force for alloy formation could be the high free energy of formation for the well-defined intermetallic compound Pt_3Zr. Ott and Raub (33), who studied this reaction with reference to corrosion phenomena, found that alloying started at about 820°C via the formation of a fcc solid solution Pt_{1-x}-Zr_x, up to a limiting value of 25 wt% zirconium at high temperatures, where there was evidence of the intermetallic compound Pt_3Zr being formed. In the catalysts of present study (Fig. 3) alloy phases due to $Pt_{11}Zr_9$ and PtZr were observed (34) in PZ-1 (wt% of Zr = 0.5) and in PZ-2 (wt% of Zr = 1.0) and in PZ-3 (wt% of Zr = 2.0) and in PZ-4 (wt% of Zr = 4.0) these phases became X-ray amorphous and peaks due to ZrO_2 were observed (34). These strong reflections, other than those of Pt_3Zr, may be because of the excess amount of zirconia present in the catalyst mass. Szymanski and Charcosset (9) have shown from ESCA and AES studies that the catalysts, even after exposing to air after preparation, indicated the presence of both zero-valent zirconium and platinum. At least in the metallic particles the zirconium is present in the metallic state and not as a platinum–zirconium–oxygen solid solution phase. The reaction (reoxidation) which may take place in air under atmospheric conditions is confined to the surface of the alloy particles.

The crystallite sizes calculated from XRD and H_2 chemisorption are presented in Table 1. For the samples for which it has been possible to calculate crystallite sizes from XRD, they are in good agreement with those calculated from H_2 chemisorption. An increase in crystallite size can be observed when compared between Pt/C and Pt-*M*/C alloy catalysts. Among alloy catalysts the crystallite size is increasing with the increase in second metal loading. This may be attributed to an increase in the apparent Pt particle size or Pt-*M* alloy or segregated second metal phases.

Electron Spin Resonance (ESR)

The ESR spectra of Pt-V/C alloy catalysts recorded at ambient temperature are shown in Fig. 4. The samples were evacuated (10^{-6} torr) at 200°C and then cooled to room temperature before recording the ESR spectra. The samples were reduced in flowing hydrogen and subsequently evacuated at 500°C did not reveal any ESR signal. Moreover, it may be mentioned that the support carbon and 5 wt% Pt/C did not exhibit any ESR signal at the same pretreatment (evacuation to 10^{-6} torr for 6 h at 200°C) and recording (at 25°C) the conditions employed in this study. A broad resonance absorption corresponding to vanadium +4

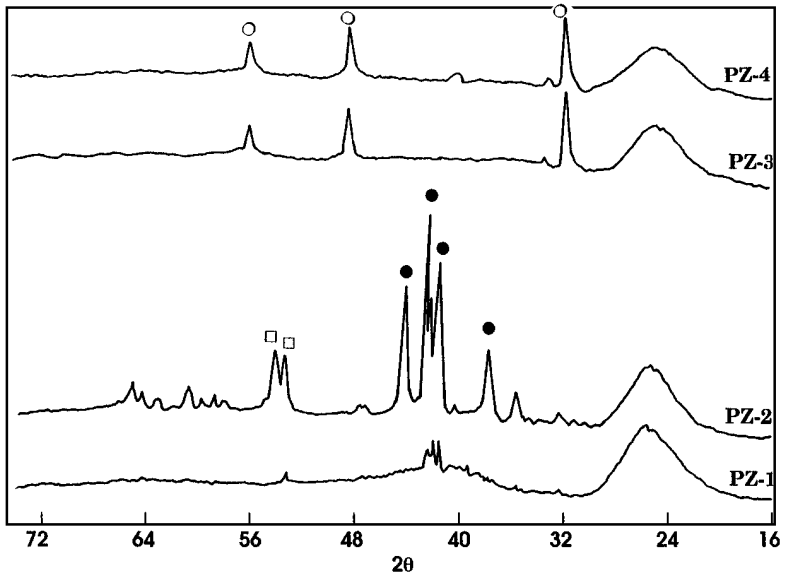

FIG. 3. X-ray diffraction patterns of Pt-Zr/C catalysts reduced at 1200°C: PtZr (●), Pt11Zr9 (□), ZrO_2 (❍).

TABLE 1

Preparation and Chemisorption Data along with BET Surface Areas and Crystallite Sizes of Pt/C and Pt-M/C Alloy Catalysts

Catalyst	Composition (wt%)	Treatment history	H_2 uptake μ mol · g^{-1}cat	H[a] / Pt	BET S A m^2g^{-1}-cat		Active site density[b] (nm^{-2})	D_HO[c] nm	D_x[d] nm
					Before alloying	After alloying			
PC-1	5 Pt	250, H_2	81.7	0.64	228	—	0.432	0.13	—
PR-1	5 Pt 0.5 Cr	760, H_2	26.7	0.21	225	192	0.134	4.1	—
PR-2	5 Pt 1.0 Cr	760, H_2	22.3	0.17	219	178	0.129	4.9	4.8
PR-3	5 Pt 2.0 Cr	760, H_2	17.8	0.14	184	131	0.136	6.0	5.2
PR-4	5 Pt 4.0 Cr	760, H_2	15.2	0.12	160	111	0.101	7.1	6.5
PV-1	5 Pt 0.5 V	960, H_2-N_2	23.2	0.18	220	211	0.141	5.0	—
PV-2	5 Pt 1.0 V	960, H_2-N_2	19.6	0.15	214	183	0.134	5.5	5.1
PV-3	5 Pt 2.0 V	960, H_2-N_2	17.9	0.14	209	159	0.112	6.0	5.8
PV-4	5 Pt 4.0 V	960, H_2-N_2	9.8	0.08	170	118	0.081	11.0	9.9
PZ-1	5 Pt 0.5 Zr	1200, H_2-N_2	20.1	0.16	223	178	0.168	5.4	—
PZ-2	5 Pt 1.0 Zr	1200, H_2-N_2	17.9	0.14	210	160	0.151	3.5	4.5
PZ-3	5 Pt 2.0 Zr	1200, H_2-N_2	13.4	0.10	199	147	0.163	4.7	—
PZ-4	5 Pt 4.0 Zr	1200, H_2-N_2	8.9	0.07	184	129	0.165	6.1	—

[a] Number of hydrogen atoms chemisorbed to total number of Pt atoms.
[b] This is equal to the number of hydrogen atoms chemisorbed per unit area of the catalyst.
[c] D_H = crystallite size calculated from H_2 chemisorption.
[d] D_X = Crystallite size determined from XRD.

oxidation state can be seen in Fig. 4. The intensity is maximum in case of PV-2 (wt% of V = 1.0). The spectrum in case of PV-1 (V wt% = 0.5) is broad. This may be because most of the vanadium appears to be consumed in alloy formation and the available free vanadyl species may be less, thus giving rise to a weak ESR signal. It can also be seen from Fig. 4 that the spectrum becomes diffused at higher vanadium loading (PV-3 = 2 wt% V and PV-4 = 4 wt% V). The hyperfine splitting corresponding to V^{4+} (S = 1/2,I = 7/2) are not observable in the spectra due to the possible spin–spin interaction between adjacent V^{4+} species in V_2O_5 spectrum. The line shape was nearly lorentzian. The g tensor of PV-2 ($g = 1.9727$) and the line width expressed by maximum slope separation H_{msl} (79 G) are close to those of pure V2O5 ($g = 1.98$), ($H_{msl} = 85$ G). The leftover vanadyl species after alloying in the PV-2 sample may be in a highly dispersed form, giving rise to this spectrum which has been attributed by various researchers to a V^{4+} ion, which exists in the non-stochiometric compound V_2O_5 formed by partial reduction (35). The absence of ESR signal for reduced sample shows that the vanadyl species in the presence of platinum are being reduced completely to V^0 and perhaps to V^{+3} and V^{+2}. This observation in ESR study shows that apart from alloy ensemble sites Pt^0 as well as V^0 sites may also separately exist on the surface. Although it is not a definitive proof for this model this is evidence for the promotional effect of reduction of VO_x species by platinum. However, the absence of hfs at room temperature may be explained as due to shorter relaxation times arising due to very closely spaced ground and exited states (36,37).

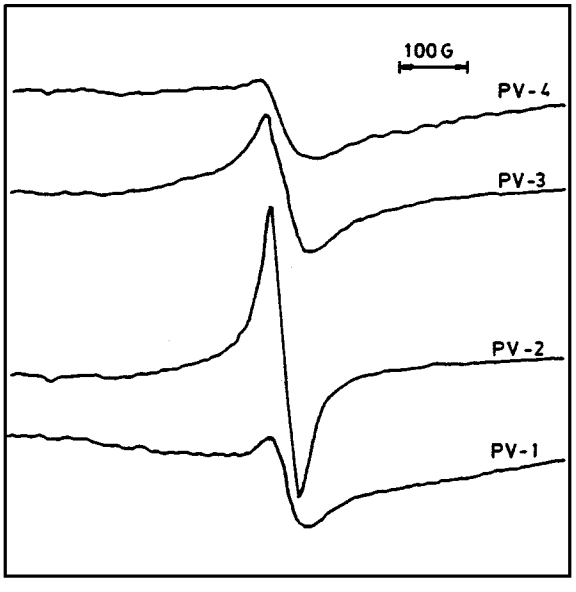

FIG. 4. Electron spin resonance spectra of Pt-V/C catalysts obtained at 25°C.

The ESR parameters, namely axially symmetric g values $g_\perp$ and $g_\parallel$ calculated from spectra, H representing the peak to peak line width along with g_{av} values are listed in Table 2 as a function of catalyst composition. The decrease in the H at higher vanadium loading may be due to the possible interaction or spin–spin pairing of the adjacent V^{4+} species. The maximum H at 1.0 wt% V (PV-1) catalyst may be due to V^{+4} species in highly dispersed form. Beyond this loading

TABLE 2

ESR Parameters of V^{4+} Species in Pt-V/C Alloy Catalysts

Catalyst	Composition (wt%)	$g_\perp$	$g_\parallel$	g_{avg}	ΔH
PV-1	5Pt 0.5 V	1.9578	2.0055	1.9896	115
PV-2	5Pt 1.0 V	1.9727	2.0142	2.0004	73
PV-3	5Pt 2.0 V	1.9395	2.0151	1.9899	135
PV-4	5Pt 4.0 V	1.9235	2.0215	1.9888	176

the decrease in H value may be due to the formation of V_2O_5 agglomerates at the expense of V^{4+} species. It is also possible that the lower oxidation states like V^{3+} which are not observable at 25°C may also be present on the catalyst surface. It is known that the isolated vanadyl species exist in tetrahedrally coordinated form, whereas the polymeric vanadyl species (agglomerates) exist in octahedrally coordinated form (35). The same coordinations can be ascribed to the sites present in PV-1, PV-2 and PV-3, PV-4 samples, respectively. The ESR observations show that, apart from alloy sites, there exist VO_x sites which may be present in dispersed, as well as agglomerated, forms. There is a chance of VO_x species encapsulating alloy sites.

Carbon Monoxide Chemisorption

Table 1 presents preparation and chemisorption data along with crystallite size of 5 wt% Pt/C and Pt-M/C alloy catalysts. CO, H_2 chemisorption, and phenol and benzene hydrogenation activity data obtained from the control experiments on 5 wt% Pt/C at 760, 960, and 1200°C are presented in Table 3. It can be seen in Table 3 that at 250 and 400°C, CO uptake was 54.8 and 58.4 μmol g^{-1}cat., respectively. On the otherhand, with increasing reduction temperatures, i.e., at 760,960, and 1200°C CO uptake continuously decreased, which shows that considerable sintering of Pt/C has occurred at these temperatures. The CO uptake at 760°C for Pt/C was 45 μmol g^{-1}cat. Whereas for Pt-Cr/C catalysts reduced at the same temperatures, it ranged between 46.1 to 20 μmol g^{-1}cat., showing a decrease in CO uptake with increasing Cr loading. Similarly, CO uptake at 960 and 1200°C was 34.3 and 22.4 μmol g^1cat., respectively. In case of Pt-V/C catalysts reduced at 960°C, CO uptake was between 49.1 to 9.8 μmol g^{-1}cat. and it decreased with increasing V loading. For Pt-Zr/C catalysts reduced at 1200°C CO uptake was between 43.7 and 9.8 μmol g^{-1}cat. and it decreased with increasing Zr loading. Similar observations were made in case of H_2 chemisorption. For a Pt/C catalyst reduced at different temperatures H_2 uptake was same at 250 and 400°C (81.7 μmol g^{-1}cat.) and it decreased with increasing reduction temperatures at 760 (50.5 μmol g^{-1}cat.), 960 (37.2 μmol g^{-1}cat.), and 1200°C (24.5 μmol g^{-1}cat.). In case of Pt-Cr/C catalysts reduced at 760°C H_2 uptakes ranged between 26.7 to 15.2 μmol g^{-1}cat. for 0.5 to 4 wt% Cr loading. For Pt-V/C and Pt-Zr/C catalysts reduced at 960 and 1200°C, H_2 uptakes were between 23.2 to 9.8 and 20.1 to 8.9 μmol g^{-1}cat., respectively, for 0.5 to 4 wt% V, Zr loading. A close observation of these results shows that the chemisorption behavior in Pt–alloy catalysts is not entirely due to sintering at the high temperatures that are used, but also it is the result of second metal addition. If the chemisorption behavior in Pt–alloy catalysts is entirely due to sintering, then the CO and H_2 uptakes of Pt-Cr/C catalysts should be equal to the CO and H_2 uptakes obtained for Pt/C reduced at 760°C. Similarly, the CO and H_2 uptakes of Pt-V/C and Pt-Zr/C catalysts should be equal to the CO and H_2 uptakes obtained for Pt/C reduced at 960 and 1200°C, respectively. In case of Pt/C catalyst reduced at different temperatures H_2 and CO uptakes become almost equal at these high temperatures (760–1200°C). Interestingly, the H_2 uptakes obtained in case of alloy catalysts is less when compared to Pt/C catalyst reduced at the same temperatures (760–1200°C), which may be due to H_2 spillover in case of Pt/C catalyst (24,38). This observation in case of Pt–alloy catalysts was attributed to a dilution effect caused with the addition of the second metal, which may result in a decrease in H_2 spillover. Similarly, higher CO uptakes were obtained in the case of Pt-alloy catalysts when compared with Pt/C catalyst reduced at high temperatures (760–1200°C). This

TABLE 3

CO and H_2 Uptake, TOF Values in Phenol Hydrogenation and Benzene Hydrogenation of 5 wt% Pt/C Reduced at Different Temperatures

Temperature (°C)	CO uptake μ mol · g^{-1}-cat.	H_2 uptake μ mol · g^{-1}-cat.	TOF in phenol hydrogenation TOF × 10^{-2} @ 200°C mol · s^{-1}Pt-site^{-1}	TOF in benzene hydrogenation TOF × 10^{-3} @ 100°C mol · s^{-1}Pt-site^{-1}
250	54.8	81.7	83	115
400	58.4	81.7	85	110
500	58.4	82.0	87	114
760	45.0	50.5	123	112
960	34.3	37.2	156	116
1200	22.4	24.5	214	109

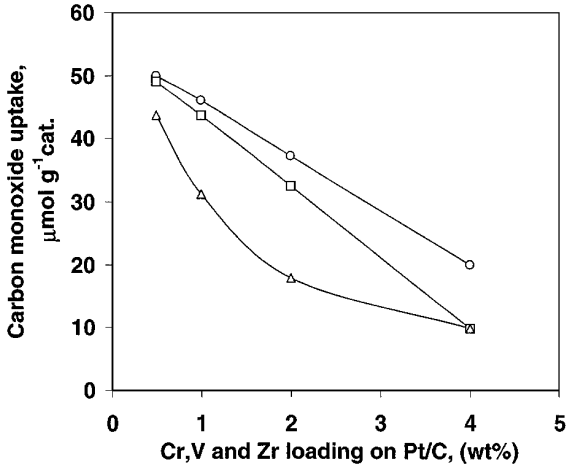

FIG. 5. CO uptake as a function of Cr, V, and Zr loading in Pt/C catalyst at 25°C: Pt-Cr/C (○), Pt-V/C (□), Pt-Zr/C (△).

shows that a considerable amount of CO is chemisorbed in a bridged mode on Pt/C catalyst, where as CO is chemisorbed predominantly in a linear mode in Pt–alloy catalysts because of the dilution of Pt sites by the second metal.

The trends in the CO uptake with increasing *M* (Cr, V, or Zr wt%) are depicted in Fig. 5. A general trend is observed where CO uptake decreases with the addition of *M*. This implies that the number of exposed Pt sites has been decreased. The decrease in CO uptake follows the order Pt-Cr > Pt-V > Pt-Zr. An important consideration in interpreting CO chemisorption behavior is that bridge-bonded CO could be present on the monometallic catalyst. Dorling and Moss (39) found that on Pt/silica catalysts CO chemisorption data in conjunction with XRD and electron microscopy showed that the ratio of Pt surface atoms/CO molecules adsorbed varied from 1 to 2 with the increase in the Pt loading of the catalysts, which modified the size of the Pt particles. Hence, some bridge bonding could lead to smaller CO/Pt values as compared to H/Pt values, assuming a H/Pt value of 1. We found that on monometallic Pt/carbon catalyst some CO was adsorbed in bridged mode of chemisorption (40). In Pt–alloy catalysts, bridge bonding (or multiple bonding) sites for CO on Pt could be blocked by the second metal, forcing CO to adsorb in a linear manner in the alloy catalysts. Palazoo *et al.* (41) reported that the presence of the second metal *M* could prevent CO bonding to multiple Pt sites due to a geometric effect, as observed from infrared spectroscopic studies. CO seems to be less sensitive to the Pt ensemble size and may represent a more suitable probe molecule for measuring exposed Pt surface sites in alloy catalysts as long as there are no chemisorption-induced surface segregation effects. Chemisorption-induced surface segregation of one of the metals in a alloy system under certain gaseous environments has been observed before. Bouman (42), in his publication dealing with surface enrichment in alloys, has discussed the environment of Pt in Pt-Au alloys when exposed to CO. This enrichment would lead to increased Pt-CO bond formation which would lead to a lower surface energy, as Au or Sn does not chemisorb CO to the extent that Pt does. But the extent of this kind of phenomenon could exist in small bimetallic particles dispersed on a support is difficult to predict. De Jong *et al.* (43) in their infrared investigation of Pt-Ag alloy particles supported on SiO_2 found that after reduction of the alloy particles and subsequent adsorption of CO the IR band tended to increase its intensity as a function of time up to 30%. This could be due to enrichment of Pt induced by CO chemisorption. If this phenomenon of surface enrichment was present it could change the nature of surface atoms in a bimetallic/alloy system, depending on the type of gas adsorbed. The nature of catalyst preparation, metal loading, and the type of support could play a part in the kind of electronic interactions possible between the two metallic components of the catalyst. This could partially explain the results obtained with various adsorbates.

Hydrogen Chemisorption

H_2 uptake values are plotted as a function of the second metal (*M*) loading in Fig. 6. It can be seen from the figure that a big drop in H_2 uptake values is taking place upon the addition of *M* to platinum. However, on the continued addition of second metal, though, H_2 uptake values are decreasing; the variation among alloy catalysts is less, when compared with the monometallic platinum catalyst. A general decrease in H_2 chemisorption capacities can be ascribed to dilution of platinum surface sites, which makes some of the platinum sites inaccessible to hydrogen to chemisorb. Additionally the variation in H_2 chemisorption among alloy catalysts may have been caused by enrichment of the second metal to the surface of the catalyst because it may tend to migrate over to the surface of Pt-*M* ensembles and

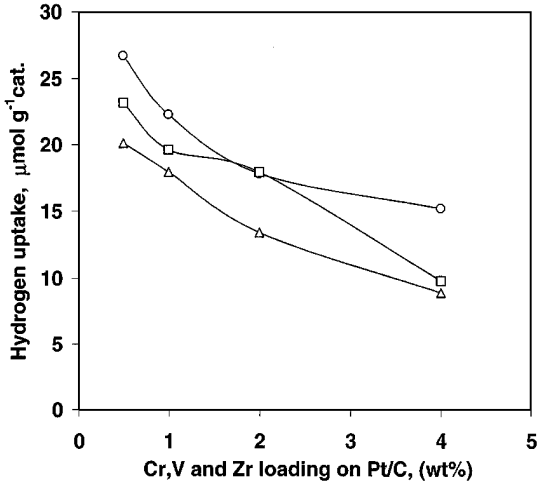

FIG. 6. H_2 uptake as a function of Cr, V, and Zr loading in Pt/C catalyst at 25°C: Pt-Cr/C (○), Pt-V/C (□), Pt-Zr/C (△).

possibly cover the platinum surface, thereby decreasing H_2 chemisorption. It is well known that H_2 dissociatively chemisorbs on platinum at ambient temperature requiring adjacent surface sites of platinum (44–46). With more and more second metal being added, fewer Pt ensembles capable to dissociate H_2 may be left and thereby rendered inaccessible for hydrogen to chemisorb. The difference in the trends of the uptake of H_2 and CO with increasing second metal loading may be attributed to the following reasons. CO adsorption on Pt is known to be associative and consequently a single Pt site would suffice to accommodate an adsorbed CO molecule. Alloying or addition of a second metal could lower such adjacent Pt sites, and, therefore, hydrogen may not be able to adsorb to the same extent as CO on bimetallic/alloy catalysts. Verbeek and Schatler made similar observations on unsupported Pt-Sn alloys (47). They found that a lesser amount of deuterium was adsorbed on Pt-Sn alloys, compared to CO and that the alloys adsorbed both the adsorbates to a lesser extent than pure platinum. Alexeev *et al*. (48) reported that in case of MgO-supported Pt-W catalysts prepared from organometallic precursors, the addition of W to Pt resulted in a reduction of chemisorption of CO and H_2, with the reduction in chemisorption being greater for catalysts prepared from organometallic precursors than those prepared from a combination of respective monometallic precursors. Passos *et al*. (49) have studied the effect of In and Sn on adsorption behavior and hydrogenation activity of Pt/Al_2O_3 catalysts. The presence of these two promoters decreased H_2 and CO chemisorption. They ascribed the chemisorption behavior to a geometric effect in which the number of contagious Pt atoms is decreased by dilution with Sn or In; i.e., the ensemble size decreases and any electronic properties play a minor role.

The overall trend in the H/Pt ratio seems to indicate that, on alloying of Pt with *M*, a drop in H/Pt value takes place and it continues to decrease although marginally with increasing *M* (Cr, V, and Zr) loading as presented in Table 1. It is interesting here to observe among Pt-M/C alloy catalysts that although Pt dispersion did not change much, on adding more *M*, site modification by the second metal becomes significant. In their work on $Pt\text{-}M/Al_2O_3$ bimetallic catalysts containing posttransition metals, viz. Te, Sb, Sn, Cheng *et al*. (50) found that, on adding the second metal, there was a dramatic decrease in H/Pt and CO/Pt ratio. Although at low contents in the catalysts some electronic effects could be detected, for posttransition metal/Pt ratio, larger than 0.1, the main effect appeared to be geometric in nature, causing the blocking of some of the Pt surface sites. Srinivasan and Davis (51), in their studies on $Pt\text{-}Sn/Al_2O_3$ catalysts, showed that one of the roles of tin in Pt-Sn bimetallic catalysts was to aid in maintaining the dispersion of platinum. The extent of the reduction of tin and the fraction of platinum in an alloy form phase depends upon the Sn/Pt ratios, surface area, and nature of the support material. From Table 1 it can be noted that a decline in the BET surface areas is taking place after heat treatment. This observation is expected, since upon the addition of Pt to carbon and the addition of a second metal to Pt/C will result in a decrease of total surface area because of pore blocking. Active site densities are derived from H_2 chemisorption and BET surface areas obtained after alloying. Active site densities (Table 1) are fairly constant in alloy catalysts and this is expected as they are derived from H_2 chemisorption data. The H_2 chemisorption depends on surface electronegativities, which are a measure of the ability of a chemically bonded atom to attract electrons towards itself (52,53). Charge transfer is an important component in surface metal–metal bonds that involve dissimilar elements (54). The decrease in the electronegativity from Pt towards the d-block elements used is the cause of decline in H_2 chemisorption. But it is clear from this study that the H_2 chemisorption method can be used to estimate the number of dispersed Pt surface sites in the alloy catalysts.

Oxygen Chemisorption

The O_2 capacities showed a very different trend as compared to that of CO and H_2 (Fig. 7). The O_2 uptake increased with increasing Cr, V, and Zr wt% loading. In the case of $Pt\text{-}Au/SiO_2$ catalysts where the effect of gold on platinum has been observed to be mainly geometric in nature, it was determined that with increasing gold contents in the catalyst the amount of O_2 adsorbed tended to decrease in a fashion similar to variations in the H_2 and the CO gas uptakes (55). The increase in the alloy catalysts with increments of the second metal could be due to several factors. One reason is that the chemisorption stoichiometry of O_2 adsorption on Pt surface atoms may be modified due to the addition of the second metal. This change in chemisorption stoichiometry could be due to the electronic modification of Pt atoms in

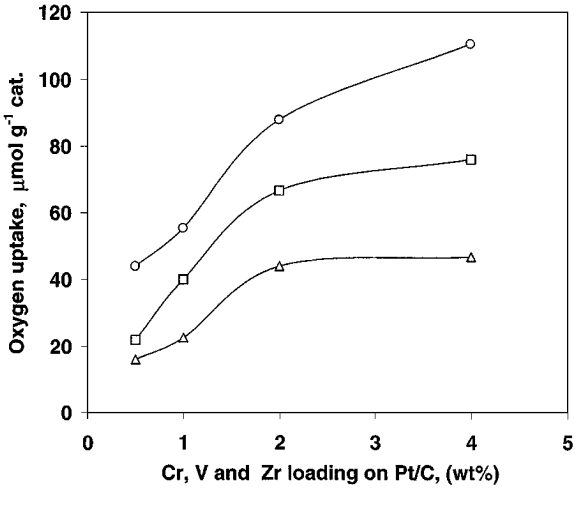

FIG. 7. O_2 uptake as a function of Cr, V, Zr loading in Pt/C catalyst at 25°C: Pt-Cr/C (○), Pt-V/C (□), Pt-Zr/C (△).

close vicinity of the second metal ions with various oxidation states. Another reason could be that the second metal may be present in lower valancy states or metallic form either independently or as Pt-*M* alloy. Metallic V and Cr and Zr or reduced species could chemisorb O_2 at room temperature. These above factors lead to larger O_2 uptakes, compared to a monometallic platinum catalyst. As the amount of second metal increased one could argue that more and more second metal could go into the reduced state. But specifically in case of Pt-V/C catalysts ESR results revealed surface VO_x species. Hence, there is an overall possibility of the second metal getting oxidized and attaining higher stable oxidation states when coming into contact with adsorbed O_2. On the other hand, considering the fact that Pt-*M* alloys are formed, the individual components in the alloy could conceivably chemisorb O_2 differently, compared to the chemisorption on the individual metal components if they were present in an unalloyed form. The individual O_2 chemisorption capacities of the alloy system prepared by us shows the trend Pt-Cr > Pt-V > Pt-Zr. This is due to increasing reducing capability of Cr and V and also depends on the order of their respective atomic size. The increasing uptake of O_2 with increasing *M* wt% loading of the alloy catalysts as observed in our study could also be a result of spillover of O_2 from platinum to the second metal. Nishiyama *et al*. (56) found that bimetallic Rh-Sn/Al_2O_3 showed a greater O_2 uptake at room temperature than the combined uptakes on the monometallic catalysts. This was attributed to the formation of Rh-Sn alloys, where the tin atoms may behave like an O_2 reservoir. It was proposed that such a close interaction between the two metals possibly leads to the spillover of oxygen from the Rh to the Sn sites and increases the oxygen uptake. The monometallic 5% Pt/carbon catalyst gave an O/H ratio of 0.6. This shows that the extent of O_2 uptake at saturation is lower than that of H_2 at saturation. Boudart and co-workers (44) have made a detailed study of H_2 and O_2 adsorption on unsupported Pt powder and found that the O/H ratio was 0.65. Hence, an O/H ratio in this range appears to apply for both supported and unsupported samples. One reason given for lower oxygen uptake on monometallic catalyst is the relative immobility of the oxygen layer as compared to hydrogen (57). The amount of weakly adsorbed oxygen is very small and this shows that oxygen is much more strongly held than hydrogen at room temperature. The complexities involved in CO chemisorption (determination of linear and bridged CO) and O_2 chemisorption (bulk oxide formation, possibility of O_2 chemisorption on the second metal) make H_2 chemisorption method more relevant to estimate apparent Pt dispersion and particle size in the alloy catalysts. This is because of the standard stoichiometry of H/Pt as unity and the blocking of migration of H_2 on alloy catalysts will also restrict the complications usually arising from H_2 spillover.

Ammonia Chemisorption

NH_3 has been widely employed as a basic adsorbate to count the number and strength of acid sites on various solid surfaces (58,59). NH_3 has been selectively used because all types of acid sites on the catalyst surface are easily accessible to NH_3 (diameter 0.26 nm) and it selectively adsorbs on sites of different strengths. It has been shown that the values of acidity obtained by ammonia adsorption (for example, the amount of NH_3 irreversibly adsorbed at a pressure of 300 mm Hg at 25°C) agree well with those obtained by other techniques such as *n*-heptane/*n*-butyl amine titrations and also with potentiometric titrations (60–62). The NH_3 chemisorption method was also used for carbon system and metal surfaces (61,62). The nature and strength of various acidic sites can directly influence and may be related to the activity and selectivity of the catalyst (63). The NH_3 uptake increased with the addition of *M* to monometallic platinum catalyst (Fig. 8). Carbon alone showed 491 μmol of NH_3 uptake, whereas monometallic 5 wt% Pt/C showed 288 μmol per gram of catalyst. This decrease can be attributed to the blocking of acidic sites containing pores by platinum. The NH_3 adsorption capacities of alloy catalysts is increasing in the order Pt-Cr > Pt-V > Pt-Zr. The NH_3 uptake increased with increasing in Cr, V, and Zr loading, respectively. The total acidic nature of the alloy catalysts may be contributed by MO_x and PtO_x species as well as carbon surface functional groups. Comparatively the low acidic character of Pt-Zr/C corresponds to the basic character of zirconium and ZrO_x species which are existing on the surface as shown from X-ray analysis. The observations show that, upon addition and alloying of Pt/carbon with Cr, V, and Zr, the acidic strength of the catalyst increases. This shows significant influence of Cr, V, and Zr and their corresponding MO_x species on the chemisorption and

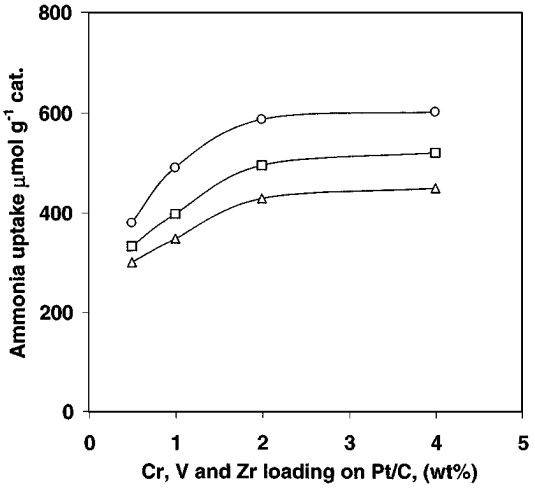

FIG. 8. NH_3 uptake as a function of Cr, V, and Zr loading in Pt/C catalyst at 25°C: Pt-Cr/C (○), Pt-V/C (□), Pt-Zr/C (△).

catalytic behaviour of Pt/carbon upon alloying. On the other hand, carbon support presents more acidic surface compared to Pt/C and Pt–alloy catalysts because the catalysts, specifically the alloy catalysts, were subjected to high temperature treatments in a reducing atmosphere. After these treatments the support surface becomes clean and the oxygen surface groups are removed.

Now we present a mechanism for Pt-*M* alloy formation on the basis of characterization of Pt-M/C alloy catalysts prepared in this study. It is possible that the organometallic compounds which are impregnated on to 5 wt% Pt/C will decompose to Cr, V, and Zr during calcination and a small amount of Cr or V or Zr oxides cannot be discounted at this stage. Of particular interest here is the implication of strong metal support interaction (SMSI) occurring between reducible oxides and group VIII metals. Tauster *et al.* (64) suggested three different mechanisms for the SMSI effect: Pt encapsulation by the support, poisioning by impurities, and alloy formation. Alloy formation was shown by Tauster *et al.* (64) to be at least thermodynamically possible under the high temperature reduction treatment used in the catalyst preparation which produced the SMSI state. As shown from XRD analysis metallic (alloy) phase was present after heat treatment, even with some air exposure of the catalyst prior to XRD analysis. It is interesting to note the absence of carbide and any intermediate phase during reduction. Other possible reduction products would be suboxides of *M*. However, compared to the thermodynamics for the formation of the intermetallics the reduction of MO_x to a suboxide is much less favourable (64). It is quite likely that the partial reduction of MO_x will create small concentrations of various suboxides as intermediates; however, the energetics favor complete reduction and alloying, given sufficient temperature and time. The results of this study provide definite evidence that alloy formation occurs when the Pt-*M* impregnates are heated in a reducing atmosphere. The temperature we employed in this study for alloying were at least 200°C higher than the usual SMSI reduction temperature (500°C). It is suggested that high temperatures are required due to the fact that impregnation of *M* in Pt/C does not necessarily result in a physical contact between all the Pt and MO_x and the high temperatures will promote Pt migrating to find MO_x. It seems reasonable to consider the possible role of alloy formation in SMSI chemistry, given that alloy formation is thermodynamically favoured at 500°C and that alloy formation has been observed directly at 700°C and higher temperatures in case of Pt-Cr/C, Pt-V/C, and Pt-Zr/C, respectively. It can be envisioned that MO_x reduction occcurs locally around Pt crystallite with simultaneous alloy formation; the alloy phase becomes partially embedded in a MO_x matrix as a consequence of the counterdiffusion of Pt and *M* atoms that occur with this simultanious process. The embedding of alloy phase causes the Pt/*M* surface ratio to decrease and *M*O character to appear at the surface which is indicated from ESR and XRD analysis. The extent to which the alloy is encapsulated depends on the temperature and time of reduction. The metal surface that is left exposed is the Pt*M* alloy surface but not a pure Pt surface. Many different approaches have been proposed to explain alloying and the consequent effects, the ensemble effect being most popular and clearly recognized. Monte-Carlo simulations and other theoretical approaches have been used to show selective segregation of additive/promoter to specific sites such as corners and edges on the alloy surface to estimate the probability of forming ensembles with different number of atoms. Coq *et al.* (65) applied a site segregation model to explain differential effects of Ga and Ge on the properties of bimetallic Rh catalysts. Recently Joyner and Shpiro (66,67) suggested a different model by surface studies of various Pt alloys that revealed the formation of sandwich structures in the surface layers, with the top layer consisting entirely of platinum and the second layer enriched in the additive. The Joyner–Shpiro model explains Pt promotion by additives as due to an electronic interaction between Pt, which comprises exclusively the outer surface layer, and the second component, which is enriched in the immediate subsurface layer. Adsorption studies on Pt-Co and Pt-Ti (8,68) alloy surfaces show that alloying will reduce the strength of chemisorption of CO on these surfaces below that found on pure Pt. The reason for this may be a SMSI effect as reasoned by Beard and Ross (69). Kuznetsov *et al.* (70) reported in case of Pt-Sn/Al_2O_3 that the catalyst is a multicomponent; i.e., it has dispersed species that are the result of chemical interactions of Sn^{4+}, $Sn2^{+}$, and Sn^0 with the support and platinum. Srinivasan and Davis (51) provided data to show that Sn is present in one or more of the three chemical states: (1) combined with platinum to form an alloy of predominantly Pt-Sn, (2) in an oxidized state (Sn^{2+} and/orSn^{4+}) that is amorphous to X-rays, and (3) metallic tin. The distribution of tin among the three chemical states depends upon the surface area of the support and Sn/Pt ratio. We feel that these observations are true in case of Pt–alloy catalyst systems used in the present study as indicated from chemisorption and XRD, and it is expected that because of high temperatures used in the preparation of Pt-M/C catalysts, a higher fraction of Pt-*M* alloy phase, as well as the metallic phase of the second metal, must be present in the catalysts. Also, Bradford and Vannice (71) have investigated CO_2 reforming of CH_4 over Pt supported on TiO_2, Cr_2O_3, ZrO_2, and SiO_2 and found from H_2 and CO chemisorption, as well as diffuse reflection infrared Fourier transform spectroscopy (DRIFTS), that metal support interactions in reducible supports (e.g., Pt-TiO_2) create active sites in metal–support interfacial region (Pt-TiO_x). However, Goodman *et al.* (54) also have reported similar observations resulting from electronic interactions in Pd-Ti and Pd-Mo monolayer alloys. Bonding between Pt and the additive element appears to be stronger

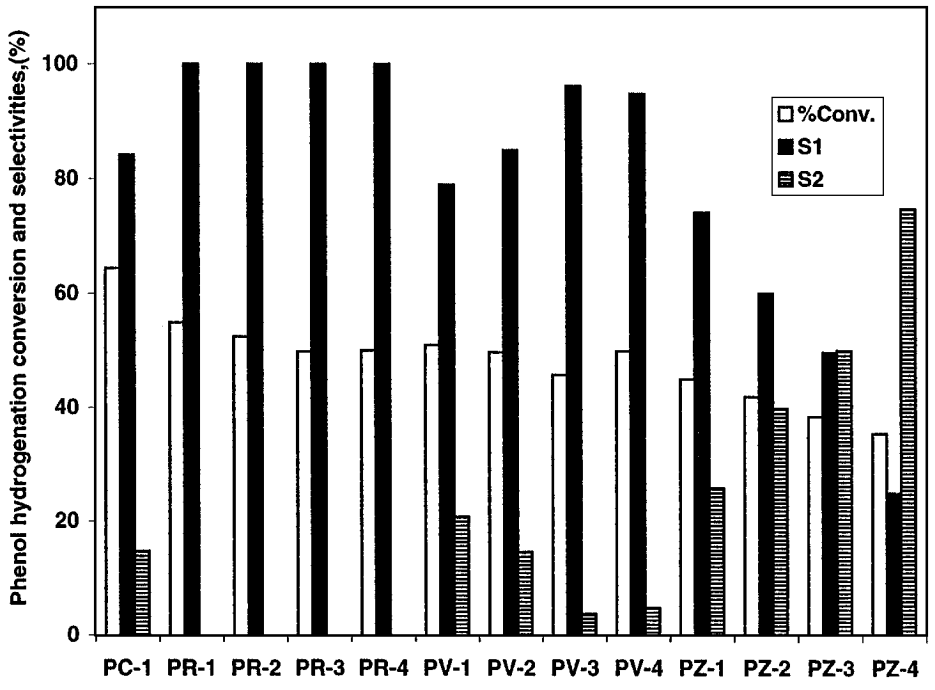

FIG. 9. Phenol hydrogenation conversion and cyclohexanone (S1) and cyclohexanol (S2) selectivities over Pt/C and Pt-M/C alloy catalysts on various catalysts at 200°C.

than that between Pt and Pt and this is an important driving force in the sandwich surface segregation. The chemisorption results suggest that an approximate sum rule may apply between (Pt-M) and (Pt-adsorbate) bond strength. The reduction of adsorption strength that is observed for CO is equally expected to occur for other adsorbates.

Phenol Hydrogenation

Phenol hydrogenation data obtained on Pt/C and Pt-*M* (Cr, V, Zr)/C catalysts is illustrated in a bar diagraph (Fig. 9). It may be mentioned here that the activity of carbon support alone in hydrogenation of phenol is practically nil under the conditions employed in this study. The reaction conditions were set on the basis of our preliminary investigations (40). It is worth mentioning here that, before the reaction runs, Pt/C catalyst was reduced at 250°C and Pt–alloy catalysts were reduced at 500°C. No significant change in TOF was observed in case of Pt/C catalyst reduced at 500°C, when compared with TOF values obtained for Pt/C catalyst reduced at 250 and 400°C (Table 3). Moreover, the reduction temperature of 250°C was not sufficient to clean the catalyst surface incase of Pt–alloy catalysts. Thus, it can also be noted that once the Pt–alloy catalysts are annealed at high temperatures during the catalyst preparation, they were reduced at low temperatures (corresponding to the Pt/C catalyst) before chemisorption and activity experiments. Thus, the Pt^0 phase in Pt/C and Pt–alloy catalysts is maintained throughout after catalyst preparation, chemisorption, and activity studies. A close comparison of H_2 chemisorption capacities and phenol conversion for the various catalysts shows that, even though a drastic decrease in H_2 uptake is taking place upon alloying of Pt/C, the variation in phenol conversion is small. The specific activity of the catalysts in terms of turnover frequency (TOF) is plotted as a function of the second metal (*M*) loading in alloy catalysts (Fig. 10). The TOF is found to increase continuously with the addition

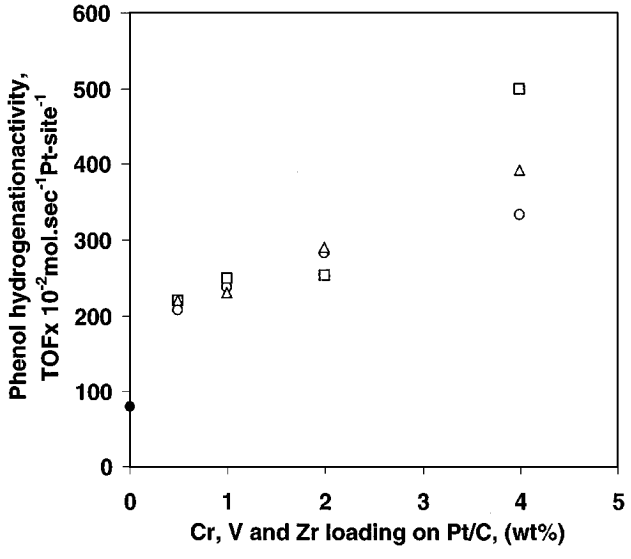

FIG. 10. TOF of phenol hydrogenation reaction for Pt/C and for Pt-M/C alloy catalysts as a function of Cr, V, and Zr loading at 200°C: Pt-Cr/C (○), Pt-V/C (□), Pt-Zr/C (△), Pt/C (●).

of the second metal loading. It can be seen that TOF of alloy catalysts in phenol hydrogenation increased significantly, compared to the monometallic platinum catalyst. On the other hand, it can be seen in Table 3 that, in Pt/C catalyst reduced at different temperatures, the TOF in phenol hydrogenation remains the same at 250 and 400°C. Beyond the reduction temperature of 400°C, i.e., at 760, 960 1200°C the TOF increased significantly. This may be due to the increase in crystallite size due to sintering of the Pt particle at these high temperatures as indicated by CO and H_2 chemisorption. Interestingly, the maximum TOF on Pt/C (obtained at 1200°C reduction temperature) will put it in the same range as the Pt-*M*/C alloy catalysts at 0.5 wt% of second metal (*M*) loading. But a clear increase in TOF values of Pt-alloy catalyst can be seen with increasing the second metal loading. Thus, the increase in TOF in case of Pt–alloy catalysts may be attributed to both crystallite size effect and the promotional effect of alloy ensembles. From these observations it appears that the intrinsic activity of the phenol hydrogenation sites on Pt/C catalyst may have increased significantly upon alloying with Cr, V, and Zr. On the other hand, the alloy formation in the catalysts may result in strong metal–metal interaction. In the SMSI state additional active sites may be created at the Pt and MO_x interface region which may also contribute to the higher activity, apart from alloy sites in the catalysts. Bradford and Vannice (71) in their study on CO_2 reforming of CH_4 found that in case of Pt supported on TiO_2, activities in terms of TOF were five times greater than Pt supported on irreducible supports like SiO_2, suggesting that active sites are created at the metal–support interfacial region. These observations by Bradford and Vannice can be applied as model to our activity results, where the SMSI-like situation exists.

Selectivity in Phenol Hydrogenation

The selectivities of cyclohexanone and cyclohexanol for various catalysts are presented in Fig. 9. In the case of 5 wt% Pt/C about 84% selectivity to cyclohexanone was obtained. Significantly on Pt-Cr/C alloy catalysts total selectivity to cyclohexanone is obtained, i.e. phenol directly hydrogenating to cyclohexanone (72). It appears that further hydrogenation of cyclohexanone to cyclohexanol is not occurring on Pt-Cr/C catalysts, unlike on monometallic platinum catalysts. Cyclohexane used as a solvent in this reaction was unaffected after the reaction (formation of benzene was not observed), confirming that dehydrogenation of cyclohexane was not occurring on the catalysts under the experimental conditions employed in this study. On Pt-V/C catalysts cyclohexanone selectivity increased from 79 to 96% with an increase in V loading from 0.5 to 4 wt% and, correspondingly, the cyclohexanol selectivity decreased. Alloying of platinum with zirconium has an opposite effect. While the selectivity decreased from 74% at 0.5 wt% Zr to 25% at 4 wt% Zr, the cyclohexanol selectivity increased from 26 to 75%, respectively. This shows that alloying of Zr to Pt has a negative effect on the cyclohexanone selectivity. No other side products were obtained along with cyclohexanone and cyclohexanol. These contrasting trends in product selectivities can be attributed to the effect of the alloying element (6). The alloy formation in the catalysts results in a strong metal–metal interaction between platinum and alloying elements. The Joyner–Shpiro model (66,67) for Pt-Cr alloying in HZSM-5 proposes a platinum enrichment at the surface with a chromium enrichment in the subsurface layer. Consequently the fraction of Pt ($\delta+$) state decreases in Pt-Cr/H-ZSM-5 with respect to Pt/H-ZSM-5. This platinum chromium electronic interaction, rather than simple dilution, is said to be responsible for both hydrogenolysis and aromatisation of lower alkanes. The platinum–chromium interaction is assumed to reduce the bonding strength between the hydrocarbon and its fragments and the metal surface with consequent activity and selectivity changes. The different activity and selectivity behavior in the hydrogenation of phenol to cyclohexanone and cyclohexanol on Pt-M/C may thus be explained as being due to different extents of platinum-metal (Cr or V or Zr) interaction affecting the Pt ($\delta+$) state and strength of bonding between the reactants and products. However, Aduriz *et al.* (73) attributed the selectivity behavior in valyene and isoprene hydrogenation to the dilution effect of palladium sites in palladium alloyed with germanium, tin, lead, and/or antimony. All alloy catalysts used in our study may oxidise in air (upon drying, upon transfer in air, perhaps also by phenol). Thus the catalysts used here are actually an alloy, with some platinum exposed, covered by CrO_x, VO_x, and ZrO_x species. Specifically these oxides may activate the -C-OH or -C=O group for hydrogenation. It is interesting to note that the most Lewis acidic additive (which is apparently present on the surface as Zr(IV) oxide) in Pt-Zr/C catalysts gives the greatest conversion to cyclohexanol. Maybe the Lewis acid activates the carbonyl towards hydride transfer by coordination-induced polarization. It is also possible that the Lewis acidic Zr(IV) promotes equilibrium reformation of the enol (cyclohexene-1-01) form of cyclohexanone, in turn promoting hydrogenation of the double bond (74).

Recently it has been reported that phenol converts to cyclohexanone, which further hydrogenates to cyclohexanol on Pt and Pd supported on Al_2O_3 and zeolite LTL (75). To understand the reaction mechanism we have carried out hydrogenation of cyclohexanone and cyclohexanol on 5 wt% Pt/C at the same reaction conditions employed in this study. In the case of cyclohexanone hydrogenation fairly good conversion towards cyclohexanol was observed, whereas in the reaction of cyclohexanol the catalyst was inactive. When we used a reaction mixture of 1 : 1 cyclohexanol and cyclohexanone more cyclohexanol formation was observed

in the product. This observation shows that the reaction passes through cyclohexanone formation. Thus, in our opinion three probable routes exist for phenol hydrogenation. First, hydrogenation of phenol to cyclohexanone and further hydrogenation to cyclohexanol. Second, direct hydrogenation of phenol to cyclohexanol and dehydrogenation to cyclohexanone. A third possible route is the formation of intermediate cyclohexene-1-ol and tautomerisation to cyclohexanone, owing to its greater stability.

The catalysts having 1 wt% Cr, V, and Zr on 5 wt% Pt/C were tested on stream for 16 h and the activity and product selectivities monitored every hour were constant. It was also observed that the catalyst deactivation follows the order Pt-Cr < Pt-V < Pt-Zr < Pt/C. Thus, Pt–alloy catalysts were found to possess longer catalyst life when compared to Pt/C catalyst. This may be attributed to the deactivation of Pt sites by coking or sintering during the reaction. Thus, it is even possible to achieve comparable TOF with a Pt/C catalyst by reducing it at 1200°C; the sintering of Pt sites will affect the catalyst life, which can be overcome by the addition and alloying of a second metal. A possible explanation for the superior performance of the Pt–alloy catalysts is that the second metals, because of their bond strength with oxygen and carbon, are localized on the surface of the crystallites, become the centers of self-poisoning, and may block the active Pt sites from poisoning. However, this is not a definitive proof for a higher resistance to deactivation of alloyed platinum with respect to pure platinum. More convincing evidence for the high poisoning resistance of alloy catalysts, compared to monometallic catalysts is the easier regeneration of catalytic activity upon pretreatment at 500°C in H_2. Thus the initial activities of alloy catalysts were regained upon prereduction. Thus by changing the alloying element (Cr, V, and Zr) and the composition of these alloy catalysts, as well as the pretreatment conditions, it is possible to tailor the structure of the metallic platinum phase. In this way catalytic activities and selectivities in the hydrogenation of phenol can be controlled in order to yield preferentially a desired product.

Benzene Hydrogenation

The rate of benzene hydrogenation has been measured on Pt/C and Pt-M/C catalysts at 100°C and atmospheric pressure. The activity of the catalysts is expressed in terms of TOF and is calculated from surface platinum atoms determined from H_2 chemisorption measurements. It is worth mentioning here that, before the reaction runs, Pt/C catalyst was reduced at 250°C and Pt-alloy catalysts were reduced at 500°C. No significant change in TOF for benzene hydrogenation was observed in case of Pt/C catalyst reduced at 500°C, when compared with TOF values obtained for Pt/C catalyst reduced at 250 and 400°C (Table 3). Moreover, the reduction temperature of 250°C was not sufficient to clean the catalyst surface in case of Pt–alloy catalysts. TOFs for

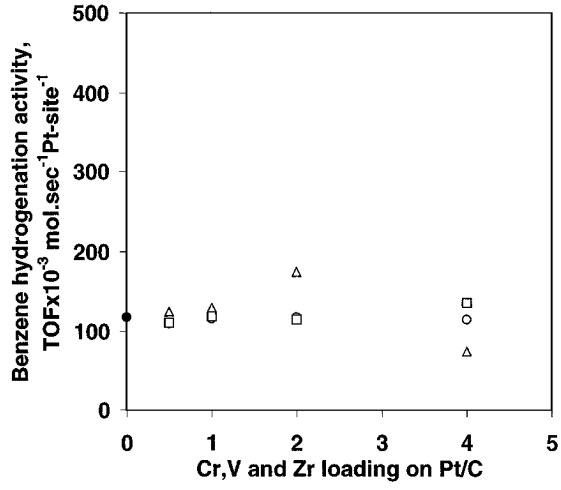

FIG. 11. TOF of benzene hydrogenation reaction for Pt/C and for Pt-M/C alloy catalysts as a function of Cr, V, and Zr loading at 100°C: Pt-Cr/C (○), Pt-V/C (□), Pt-Zr/C (△), Pt/C (●).

benzene hydrogenation are given in Fig. 11 as a function of the second metal (*M*) loading present in the alloy catalysts. The TOF of Pt-*M*/C and Pt/C catalysts are fairly constant. On the other hand, it can be seen from Table 3 that, in case of Pt/C catalyst reduced at different temperatures, the TOF in benzene hydrogenation remains the same and this observation is expected, as it is well known that benzene hydrogenation is a facile reaction. Engels and co-workers (29) found a decrease in the hydrogenation function of Pt-Cr/Al_2O_3 catalysts. In case of alloy catalysts reduction in the benzene hydrogenation rate may be because of a significant decrease in exposed platinum metal area, i.e. active platinum surface sites, from sintering/alloying during the high temperature treatment of the prepared catalysts which is reflected in case of Pt/C catalyst reduced at different temperatures. A small decrease in the benzene hydrogenation activity of Pt after alloying with small amounts of a low-activity metal, such as Zr (76), Au (77), or Cu (78), has been interpreted as evidence of structure sensitivity, but the observed changes were very small. Campbell *et al.* (79) studied the effect of deposition of Bi on benzene adsorption on a Pt(111) single crystal and concluded that reducing the Pt ensemble size first inhibited the dehydrogenation reaction and then lowered the benzene desorption temperature. Lin and Vannice (80) reasoned that, as larger ensembles exist on large Pt crystallites, particularly those associated with Pt(111) plane will result in deactivation behavior of the Pt powder, which they studied. Based on the results of Campbell *et al.* (79), low Bi coverages would hinder benzene dehydrogenation and decrease H-deficient species, thus increasing the activity, whereas at high Bi coverage benzene adsorption itself could be decreased, thus resulting in suppressed activity. This prediction is consistent with two maxima in the activity versus the metal composition observed with a series of Pt-Re/Al_2O_3 catalysts (81). Although

structure sensitivity in the benzene hydrogenation reaction has not been established, the possibility exists that the dehydrogenation/decomposition of benzene on Pt may be structure sensitive. Consequently, the final activity, based on the remaining free metal surface area, could vary significantly. The discrepancies in TOF among Pt/C, as well as Pt–alloy catalysts, can be attributed to the above reasons.

Sulfur Resistance Behavior of Pt–Alloy Catalysts in Benzene Hydrogenation

Benzene hydrogenation at 100°C, a facile reaction, has been employed to test the thiotolerance level of alloy catalysts. For high temperature reactions the catalysts are able to withstand sulfur concentrations but they are encountered by deactivation processes like coke deposition and sintering. Bengel and Ku (82) have investigated the effect of sulfur on the oxidation of CO on the (110) surface of platinum. They found that the rate of CO_2 formation was affected by the presence of sulfur on the surface. Guenin *et al.* (83) have studied resistance to sulfur poisoning of Pt/Al_2O_3 catalysts in the dehydrogenation of cyclohexane. The thiotolerance level was found to be affected by the acidity of Al_2O_3, where the carrier has been modified by K or Cl. The effect of second metal loading on the ratio of benzene hydrogenation conversion after sulfur addition to benzene and before sulfur addition to benzene is plotted in Fig. 12. It can be seen in Fig. 12 that the activity ratio is decreasing continuously with the increase in second metal loading. The overall thiotolerance level follows the order Pt-Cr > Pt-V > Pt-Zr. However, this is not a definite proof for a high sulfur resistance of alloyed platinum with respect to pure platinum because Cr or V or Zr atoms on the catalyst surface can participate in H_2S adsorption. Table 4 shows the benzene hydrogenation activity before and after sulfiding for Pt/C and 1% Pt-*M*/C alloy catalysts. It can be clearly seen from the table that while the activity of the Pt/C falls after sulfiding, retaining only 12% activity, the Pt-*M*/C alloy catalysts retain moderately higher activities in the order of Pt-Cr > Pt-V > Pt-Zr. This observation confirms the overall trends in the case of different metals alloyed with platinum. This can be further explained by the fact that not all S atoms fed with benzene are trapped during the deactivation process by metallic phase and an adsorption desorption process of S may exist before reaching the thiotolerance level. On the other hand, part of the sulfur is adsorbed on the support, besides adsorption on platinum. More convincing evidence for the higher sulfur resistance of the Pt-*M* alloy catalysts is the easier regeneration of their catalytic activity with respect to pure platinum. Treatment at 500°C in H_2 flow for 2 h could completely regenerate the activity of Pt-*M* alloy catalysts, whereas that was not possible in the case of Pt/C catalyst. Therefore, it can be concluded that Pt-S bond strength is weaker when the Pt atoms are alloyed. And, moreover, Pt-S in Pt/C is stronger than Zr-S > V-S > Cr-S and that may be the reason why the alloy catalysts could be easily regenerated. This behavior can be related to electron deficiency of Pt atoms which lower the binding energy with electrophilic adsorbates like sulfur (84). However, the intrinsic thioresistance of the active metal is not modified and poisoning is only delayed, thus increasing the lifetime of the catalyst. Similar observations were made in case of Pt/ZrO_2, Pt-ZrO_2/C, and Pt-zeolite for their easier regeneration after sulfur poisoning (85).

TABLE 4

Benzene Hydrogenation Rate for Pt/C and Pt-M/C Catalyst before and after Sulfur Poisoning

Catalyst	Benzene hydrogenation rate × 10^{-2} mol · h^{-1} g^{-1} cat. @ 100°C		
	Before sulfiding	After sulfiding	Activity retained (%)
PC-1	22.27	2.8	12.6
PR-2	17.65	12.54	71.0
PV-2	18.69	9.16	49.0
PZ-2	14.56	5.2	35.7

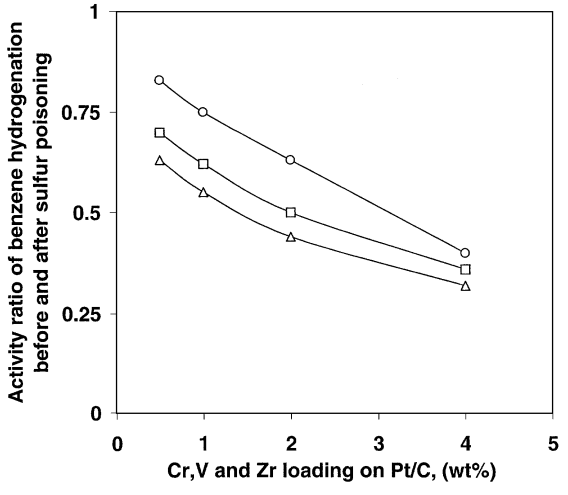

FIG. 12. Benzene hydrogenation activity ratio (activity before and after sulfur poisoning) for Pt-M/C alloy catalysts as a function of Cr, V, and Zr loading at 100°C: Pt-Cr/C (○), Pt-V/C (□), Pt-Zr/C (△).

CONCLUSIONS

1. X-ray diffraction study confirms the alloy formation in the prepared catalyst. XRD, ESR, and chemisorption studies on Pt-*M*/C alloy catalysts show that the catalyst surface actually consists of an alloy phase, metallic Pt, and *M*, along with MO_x (M = Cr, V, or Zr) phase.

2. Chemisorption studies show that the platinum catalysts upon alloying with Cr, V, or Zr exhibited loss in the Pt area; i.e. platinum dispersion, even though it is not reflected in the activity of alloy catalysts.

3. In phenol hydrogenation reaction Pt-Cr/C and Pt-V/C are found to be highly selective towards the product cyclohexanone, yielding almost total selectivity, whereas Pt-Zr/C catalysts gave high selectivity to cyclohexanol. The TOF of Pt/C catalysts was increased upon alloying. This study shows that one can tailor the metallic phase in the catalyst in order to get a desired product.

4. In benzene hydrogenation, even though a decrease in rate is observed the specific activity of alloy catalysts remains constant and at the same level as Pt/C. The sulfur resistance studies of the alloy catalysts shows that the alloy catalysts exhibit significant thiotolerance level, retaining their initial activity, unlike the monometallic catalyst.

5. The alloy catalysts exhibit their superior catalytic activity, thiotolerance level, and longer catalyst life, when compared to that of monometallic platinum catalysts.

ACKNOWLEDGMENTS

We thank both the referees for their helpful comments. We are grateful to Dr. K. V. Raghavan, Director, Indian Institute of Chemical Technology, Hyderabad, India, for his consistent encouragement. We also thank the Council of Scientific and Industrial Research, New Delhi, India for financial support in the form of Scientist pool to STS.

REFERENCES

1. Sinfelt, J. H., "Bimetallic Catalysts." Wiley, New York, 1983.
2. Shibata, M., and Masumoto, T., *in* "Preparation of Catalysis IV" (B. Delmon, P. Grange, P. A. Jacobs, and G. Poncelet, Eds.). Elsevier, Amsterdam, 1987.
3. Molnar, A., Smith, G. V., and Bartok, M., *in* "Advances in Catalysis" (D. D. Eley, H. Pines, and P. B. Weisz, Eds.), Vol. 36, p. 329. Academic Press, San Diego, 1989.
4. Joyner, R. W., and Shpiro, E. S., *Catal. Lett.* **9**, 239 (1991).
5. Jentys, A., Mc Hgugh, B. J., Haller, G. L., and Lercher, J. A., *J. Phys. Chem*. **96**, 1324 (1992).
6. Srinivas, S. T., Jhansi Lakshmi, L., and Kanta Rao, P., *Appl. Catal. A* **110**, 167 (1994). [References cited therein]
7. Srinivasan, R., Sharma, R., Su, S., and Davis, B. H., *Catal. Today* **21**, 83 (1994).
8. Bardi, U., Dahlgren, D., and Ross, P. N., *J. Catal.* **100**, 196 (1986).
9. Szyamanski, R., and Charcosset, H., *Plat. Met. Rev.* **30**, 23 (1986).
10. Jalan, V. M., Lands Man, D. A., and Lee, J. M., U.S. Patent 4,192,907 (1980).
11. Wan, C. Z., U.S. Patent 4,822,699 (1989).
12. Derouane, E. G., *J. Mol. Catal.* **25**, 51 (1984).
13. Martens, J. H. A., and Prins, R., *Appl. Catal.* **46**, 31 (1989).
14. Margitfalvi, J., Szabo, S., and Nagy, F., *Stud. Surf. Sci. Catal.* **27**, 373 (1986).
15. Travers, C., Chan, T. D., Snappers, R., and Bournon Ville, J. P., U.S. Patent 4,456,775 (1984).
16. Shastri, A. G., and Schwank, J., *J. Catal.* **95**, 271 (1985). [References cited therein]
17. Thomas, K. L., "Catalytic Processes and Proven Catalysts," p. 141. Academic Press, New York, 1980.
18. Poltarzewski, Z., Galvagno, S., Pietrpaolo, R., and Staiti, P., *J. Catal.* **102**, 190 (1986).
19. Dees, M. J., Bol, M. H. B., and Ponec, V., *Appl. Catal.* **64**, 279 (1990).
20. Gallezot, P., Fendler, A. G., and Richard, D., *in* "Catalysis or Organic Reactions" (W. E., Pascoe, Ed.), p. 1. Dekker, New York, 1992.
21. Van Peppen, J. F., Fisher, W. B., and Chan, C. H., *in* "Phenol Hydrogenation Process in Catalysis of Organic Reactions" (R. L. Augustine, Ed.), p. 355. Dekker, New York, 1980.
22. Lin, Y., Wang, I., and Yeh, C., *Appl. Catal.* **41**, 53 (1988).
23. Dodgson, I., Griffin, K., Barberis, G., Pignattaro, F., and Tauszik, G., *Chem. Ind. (London)*, 830 (1989).
24. Srinivas, S. T., and Kanta Rao, P., *J. Catal.* **148**, 470 (1994).
25. Klug, H. P., and Alexander, L. E., "X-Ray Diffraction Procedures," p. 635. Wiley, New York, 1974.
26. Delgass, W. N., and Wolf, E. E., *in* "Chem. Reaction and Reactor Engg." (J. J. Carberry and A. Varma, Ed.), p. 151. Dekker, New York, 1987.
27. Joint Committee on Powder Diffraction Files (Eds.), ASTM Card No. 4-802, Pennsylvania, 1984.
28. Joint Committee on Powder Diffraction Files (Eds.), ASTM Card No. 8-374, Pennsylvania, 1984.
29. Engels, S., Lausch, H., Peplinski, B., Wilde, M., Morke, W., and Kraak, P., *Appl. Catal.* **55**, 93 (1989).
30. Joyner, R. W., Shpiro, E. S., Johnston, P., Minachev, K. M., and Tuleouva, G., *Catal. Lett.* **11**, 319 (1991).
31. Joint Committee on Powder Diffraction Files (Eds.), ASTM Card Nos. 13-513, 18-980, and 19-918, Pennsylvania, 1984.
32. Cambins, G., and Chadwick, D., *Appl. Catal.* **25**, 191 (1986).
33. Otto, D., and Raub, Ch. J., *Metall. (Berlin)* **32**, 140 (1978).
34. Joint Committee on Powder Diffraction Files (Eds.), ASTM Card Nos. 19-920, 27-367, and 36-420, Pennsylvania, 1984.
35. Chary, K. V. R., Ph.D. thesis, Osmania University, Hyderabad, 1986.
36. Jhansi Lakshmi, L., Narsimha, K., and Kanta Rao, P., *Appl. Catal.* **94**, 61 (1993).
37. Jhansi Lakshmi, L., and Kanta Rao, P., *Appl. Catal.* **101**, 221 (1993).
38. Mahipal Reddy, B., Srinivas, S. T., and Kanta Rao, P., *Indian J. Chem*. **31**, 957 (1992).
39. Dorling, T. A., and Moss, R. L., *J. Catal.* **7**, 378 (1967).
40. Srinivas, S. T., Ph.D. thesis, Osmania University, Hyderabad, 1993.
41. Palazoo, A., Bonev, C. H., Shopov, D., Lietz, G., Sarkanay, A., and Volter, J., *J. Catal.* **103**, 249 (1987).
42. Bouwman, R., *Gold Bull.* **11**, 81 (1978).
43. de Jong, K. P., Schlenter, B. E. B., Meima, C. R., Verkerk, R. C., Lammers, M. J. J., and Geus, J. W., *J. Catal.* **81**, 67 (1983).
44. O'Rear, D. J., Loffler, D. G., and Boudart, M., *J. Catal.* **121**, 131 (1990). [References cited therein]
45. Prado-Burgvete, C., Linares-Solano, A., Rodriguez-Reinoso, F., and Salinas-Martinez, C., *J. Catal.* **128**, 397 (1991). [References cited therein]
46. Balakrishnan, K., and Schwank, J., *J. Catal.* **127**, 287 (1990).
47. Verbeek, H., and Sachtler, W. M. H., *J. Catal.* **42**, 257 (1976).
48. Alexeev, O., Shelef, M., and Gates, B. C., *J. Catal.* **164**, 1 (1996).
49. Passos, F. B., Schmal, M., and Vannice, M. A., *J. Catal.* **160**, 106 (1996).
50. Cheng, C. H., Dooley, K. M., and Price, G. L., *J. Catal.* **116**, 325 (1989).
51. Srinivasan, R., and Davis, B. H., *J. Catal.* **124**, 257 (1991).
52. Sanderson, R. T., "Chemical Bonds and Bond Energies." Academic Press, New York, 1976.
53. Reed, L. H., and Allen, L. C., *J. Phys. Chem*. **96**, 157 (1992).
54. Rodriguez, J. A., and Goodman, D. W., *Science* **257**, 897 (1992).
55. Balakrishnan, K., Sachdev, H., and Schwank, J., *J. Catal.* **121**, 441 (1990).
56. Nishiyama, S., Yanagi, H., Nakayama, H., Tsuruya, S., and Masai, M., *Appl. Catal.* **47**, 25 (1989).
57. Barth, R., Pitchai, R., Anderson, R. L., and Verykios, X. E., *J. Catal.* **116**, 61 (1989).
58. Kung, M. C., and Kung, H. H., *Catal. Rev. Sci. Eng.* **27**, 425 (1985).
59. Tanabe, K., "Solid Acids and Bases." Academic Press, Tokyo, 1970.
60. Laine, J., Yunes, S., Brito, J., and Andreu, P., *J. Catal.* **62**, 157 (1980).
61. Noh, J. S., and Schwarz, J. A., *Carbon* **28**, 599 (1990).

62. Arico, A. S., Antonucci, V., Pino, L., Antonucci, P. L., and Giordano, N., *Carbon* **28**, 599 (1990).
63. Sivaraj, C., Srinivas, S. T., Nageswar Rao, V., and Kanta Rao, P., *J. Mol. Catal.* **60**, L23 (1990).
64. Tauster, S., Fung, S., and Garten, R., *J. Am. Chem. Soc.* **100**, 170 (1978).
65. Aduriz, H. R., Bodnariuk, P., Coq, B., and Figueras, F., *J. Catal.* **119**, 97 (1989).
66. Joyner, R. W., Shpiro, E. S., Johnston, P., and Tuleuova, G. J., *J. Catal.* **141**, 250 (1993).
67. Shpiro, E. S., Joyner, R. W., Johnston, P., and Tuleuova, G. J., *J. Catal.* **141**, 266 (1993).
68. Bardi, U., Beard, B. C., and Ross, P. N., *J. Catal.* **124**, 22 (1990).
69. Beard, B. C., and Ross, P. N., *J. Phys. Chem.* **90**, 6811 (1986).
70. Kuznetsov, V. I., Belyi, A. S., Yurchenko, E. N., Smolikov, M. D., Protasova, M. T., Zatolokina, E. V., and Duplayakin, V. K., *J. Catal.* **128**, 1 (1991).
71. Bradford, M. C. J., and Vannice, M. A., *J. Catal.* **173**, 157 (1998).
72. Srinivas, S. T., and Kanta Rao, P., *J.C.S. Chem. Commun.*, 33 (1993).
73. Aduriz, H. R., Bodniruk, P., Coq, B., and Figueras, F., *J. Catal.* **129**, 47 (1991).
74. Kanta Rao, P., Jhansi Lakshmi, L., and Srinivas, S. T., "Catalysis of Organic Reactions" (M. G. Scaros and M. L. Prunier, Eds.), p. 463. Dekker, New York, 1994.
75. Talukdar, A. K., Bhattacharya, K. G., and Sivasankar, S., *Appl. Catal. A* **96**, 229 (1993).
76. Szymanski, R., and Charcosset, H., *J. Mol. Catal.* **25**, 337 (1984).
77. Puddu, S., and Ponec, V., *Recl. Trav. Chim. Pays-bas* **255**, 95 (1976).
78. Paramalina, A., Alekseev, O. S., Ryndin, G. A., Ya, A., and Giordano, N., *React. Kinet. Catal. Lett.* **32**, 199 (1986).
79. Campbell, J. M., Seimanides, S., and Campbell, C. T., *J. Phys. Chem.* **93**, 815 (1989).
80. Lin, S. D., and Vannice, M. A., *J. Catal.* **143**, 539 (1993).
81. Bolivar, C., Charcosset, H., Frety, R., Tournayan, L., Betizeau, C., Leclercq, G., and Maurel, M., *J. Catal.* **45**, 179 (1976).
82. Bonzel, H. P., and Ku, R., *J. Chem. Phys.* **58**, 4617 (1973).
83. Guenin, G., Breysse, M., Frety, R., and Barbier, J., *J. Catal.* **103**, 144 (1987).
84. Srinivas, S. T., and Kanta Rao, P., "International Series on Chemical Engineering" (P. Kanta Rao and R. S. Benival, Eds.), p. 254. Wiley Eastern, New Delhi, 1995.
85. Szyamanski, R., Charcosset, H., Gallezot, P., and Massardier, J., and Tournayan, L., *J. Catal.* **97**, 366 (1986).